Ultrafast semiconductor spectroscopy using terahertz electromagnetic pulses

Toshiaki Hattori, Satoshi Arai, Keisuke Ohta, Aya Mochiduki, Shin-ichi Ookuma, Keiji Tukamoto, and Rakchanok Rungsawang

Institute of Applied Physics, University of Tsukuba, 1-1-1 Tennodai, Tsukuba, Ibaraki, 305-8573 Japan

Abstract

Terahertz electromagnetic pulses can serve as a new and unique tool for various types of spectroscopy. We first characterized the temporal and spatial properties of THz pulses generated from a large-aperture photoconductive antena, and then used them for the study of the ultrafast dynamics of electrons in semiconductros. We studied the dynamics of electrons generated by femtosecond optical pulses with positive and negative excess energies in GaAs and InP by observing the waveform of the emitted THz radiation. Subpicosecond intraband relaxation was observed with positive excess energies. With negative excess energies, a picosecond transition from the Urbach state to free carrier states was observed.

Key words: THz radiation, imaging, gallium arsenide, indium phosphide, Urbach tail
PACS: 78.47.+p, 42.65.Re, 72.20.Jv

1 Introduction

Terahertz (THz) waves are electromagnetic radiation with a frequency ranging from 100 GHz to 10 THz, as shown in Fig. 1. This frequency region lies at the boundary of radio waves and light in the wide spectrum of the electromagnetic waves. Little studies and uses of THz waves have been done until recent years because of the difficulty in their generation, manipulation, and detection. Recent advances in the solid-state laser technology are accelerating their studies and applications.

Email address: hattori@bk.tsukuba.ac.jp (Toshiaki Hattori).

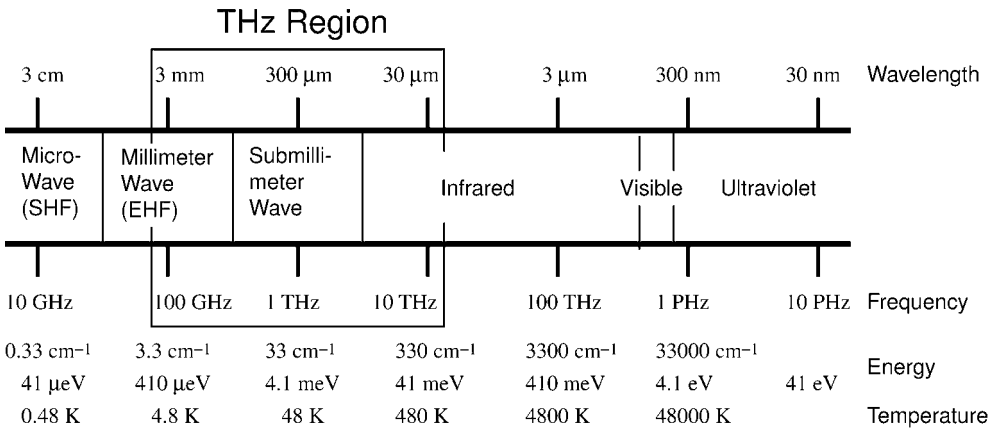

Fig. 1. Spectrum of electromagnetic waves ranging from microwaves to ultraviolet waves.

One of the most promising applications of THz waves is imaging. THz waves can penetrate through nonmetalic and nonpolar materials, such as paper, plastics, and textiles. THz waves are much safer than x-rays and can be used for identification of specific chemicals such as drugs. Applications of THz imaging for security check, product inspection, and medical diagnoses are expected.

Another and very important application of THz waves is spectroscopy. Rotational modes and intermolecular vibration modes of small molecules lie in the THz region. Other interesting spectroscopic applications of THz waves include studies of optical phonons and polaritons in polar crystals, vibrational and librational modes of large molecules and molecular crystals, localized lattice vibration of disordered systems, and plasma modes in metallic and conductive materials.

Frequency-tunable THz sources such as parametric oscillators and quantum cascade lasers have been used for spectroscopic studies of these materials. Time-domain spectroscopy is also a powerful tool for THz spectroscopy, where time-domain electric field data are used for the acquisition of frequency-domain information. Therefore, time-domain information of ultrafast processes can also be obtained using THz spectroscopy. The initial processes of photo-injected carriers in semiconductors and other materials occur in the femtosecond regime, which corresponds to THz frequencies. Since movement of charges results in emission of electromagnetic waves, observation of emitted THz waves is an important spectroscopic means for the study of ultrafast processes in these materials.

In this paper, first we describe the temporal and spatial properties of THz electromagnetic pulses generated from biased semiconductors, and then describe the results of the THz emission spectroscopy of ultrafast electron dynamics in GaAs and InP.

2 Temporal waveforms of terahertz pulses

When a sudden change in current or polarization is induced in mateirals by femtosecond optical pulses, broadband electromagnetic pulses are emitted. Since the spectra expand up to terahertz region, they are called terahertz pulses. They are used as a source for spectroscopy and imaging in this frequency region. Several methods are available for THz pulse generation, such as photoconductive switch [1], semiconductor surface emission, and optical rectification [2]. Among them, the method using a large-aperture photoconductive antenna [3–5] can provide very intense pulsed THz field, and has been used for applications that require intense field such as ionization of Rydberg atoms [6], THz-field-induced second-harmonic generation from molecular liquids [7], and real-time imaging [8–10]. Since THz pulse emitted from a large-aperture antenna has a smooth wave front, this type of THz sources are also suited for the study of temporal and spatial waveforms of the THz pulses, which is the fundamental knowledge for further uses of them.

We have studied the change in the temporal waveforms of the THz pulses emitted from a large-aperture photoconductive antenna as a function of the propagation distance, and explained the results based on diffraction integral and Gaussian beam model. Detailed description of this study is given in a separate paper [11]. The emitter was a large-aperture antenna made of semi-insulating GaAs wafer. Two electrodes were attached to the wafer, and the spacing between them was 30 mm. A pulsed voltage of 12 kV was applied to the electrodes. The emitter area between the electrodes was illuminated by amplified femtosecond optical pulses having 150-fs duration and 800-nm central wavelength. Charge carriers are created by the optical pulse radiation. They are accelerated by the applied electric bias field immediately after the creation, which leads to sudden change in the current at the surface of the wafer. The temporally changing current produces electric field. The process is described by the current surge model [12,13], and the expression for the surface field, $E_{\mathsf{surf}}(t)$, is given as

$$E_{\mathsf{surf}}(t) = -E_{\mathsf{bias}} \frac{\sigma_{\mathsf{s}}(t)\eta_0}{\sigma_{\mathsf{s}}(t)\eta_0 + 1 + \sqrt{\epsilon}}, \tag{1}$$

which shows that the field on the emitter surface is proportional to the current. Here, E_{bias} is the bias field, $\sigma_{\mathsf{s}}(t)$ is the time-dependent surface conductivity, ϵ is the dielectric constant of the emitter medium, and $\eta_0 = 377\ \Omega$ is the impedance of vacuum. It has been shown, however, that the field at positions far from the surface is proportional to the time derivative of the surface field [14]. The temporal waveform of focused THz pulse becomes proportional

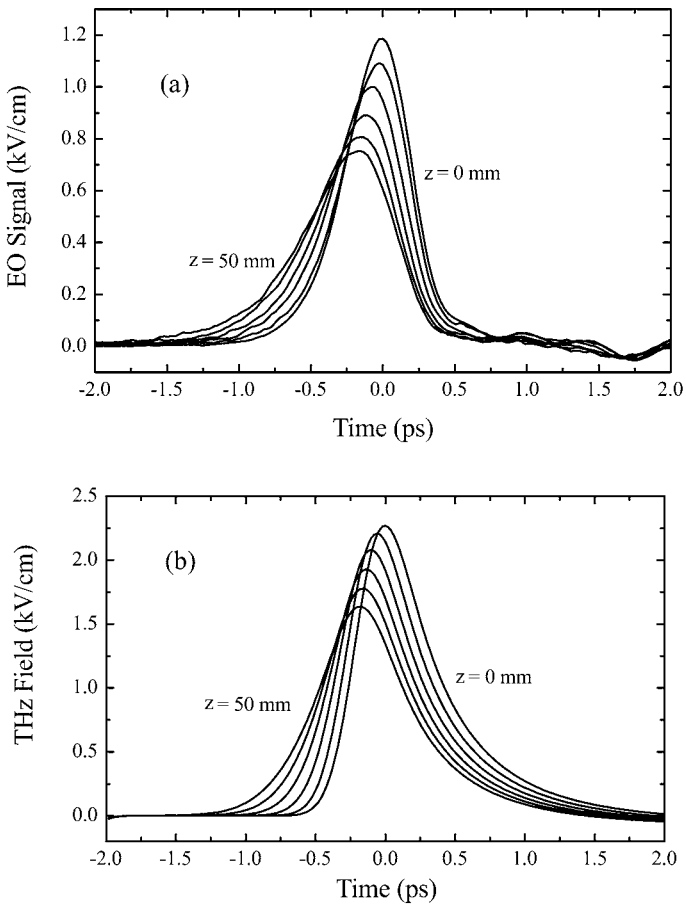

Fig. 2. Temporal field waveforms of a focused THz pulse. The observation position was change from the focus ($z = 0$ mm) to 50 mm away from the focus ($z = 50$ mm) by a step of 10 mm. (a) Experimentally obtained data. (b) Calculated data obtained by simulation assuming Gaussian-beam propagation of each frequency component.

to the far field waveform as well [11]:

$$E_{\mathrm{focus}}(t) = \frac{A^2}{2cf}\frac{d}{dt}E_{\mathrm{surf}}(t). \tag{2}$$

Here, A is the beam size and f is the focal length. The time dependence of the surface current becomes step-like function with a fast rise when the lifetime of the carriers is sufficiently long, which results in a half-cycle shape of the far field waveform. These facts show that the THz pulse experiences drastic change in the temporal waveform during propagation and focusing in the free space.

In the experiments, we focused the THz pulses emitted from the large-aperture antenna using an off-axis parabolic mirror with a focal length of 152.4 mm. The position dependence of the temporal waveform of the electric field of the THz pulses was observed using the electro-optic (EO) sampling method [15].

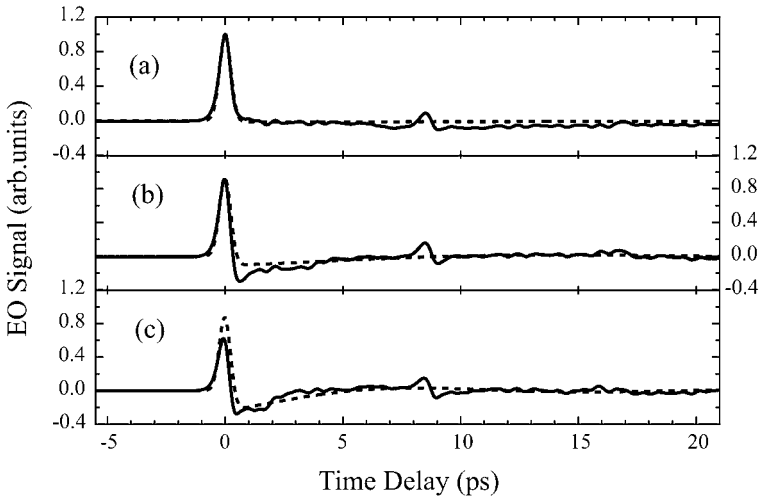

Fig. 3. Waveforms of focused THz pulses that were passed through different sizes of circular metal apertures. Solid lines are the experimental results and the dotted lines are the simulated waveforms. (a): The waveform observed with only a 1-mm-thick 8-mm-size square aperture, which was used as a crystal holder cover, in front of the EO crystal. (b) and (c): The waveforms observed with a ϕ 3.8-mm and a ϕ 2.5-mm circular aperture in front of the EO crystal, respectively.

Examples of the data obtained are shown in Fig. 2(a). All of the waveforms were observed on the propagation axis. We can see that the waveform is almost half-cycle at the focus, and is deformed significantly during the propagation. We simulated the waveform change using two methods. The first method uses the diffraction integral. The second one is based on the Gaussian beam model, where each frequency component of the THz pulse is assumed to propagate as a Gaussian beam. The results of the second method are shown in Fig. 2(b), which reproduced well the position dependence of the experimentally obtained waveform. Similar results were also obtained by the first method.

In a separate experiment [16], we observed change in the temporal waveform of THz field when the pulses are transmitted through a metal aperture. THz pulses are composed of a broad spectrum of frequency components. Each frequency component behaves in a slightly different manner, which is evident in the position dependent waveform described above. When THz pulses propagate through an aperture made of conductive materials, the frequency dependent propagation becomes more apparent because of the fact that conductive apertures behave as a waveguide, which has a cutoff frequency:

$$\nu_{\mathrm{c}} = \frac{c}{2a}, \tag{3}$$

for a square waveguide with an edge length of a, and

$$\nu_{\mathrm{c}} = \frac{1.841}{2\pi} \cdot \frac{c}{r}, \tag{4}$$

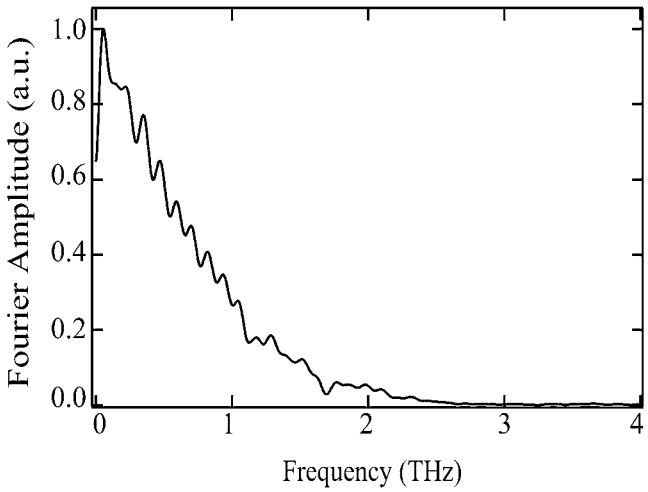

Fig. 4. Typical spectrum of the THz pulses.

for a circular waveguide with a radius of r. Here c is the velocity of light in vacuum. Components of frequency below the cutoff becomes evanescent and decays exponentially during the propagation through the aperture.

We observed the temporal waveforms of the THz pulses after propagation through a metal aperture at a position close to the aperture. The results are shown by the solid lines in Fig. 3. It is seen that a small dip is developed after the main peak due to the propagation through the aperture. The results were simulated using a simple model assuming the waveguide effect, as shown in the dotted lines in Fig. 3. These resuls show that relatively large apertures can affect the THz pulse waveforms significantly.

3 Spatial profiles of terahertz waves

The pulses emitted from photoconductive antennas have very broad spectrum extending from dc to a few THz, as shown in Fig. 4. Since the diffraction effects depend on the frequency, unique behaviors of spatial profile is observed with almost half-cycle THz pulses. The spatial distribution of the THz wave was observed using a THz imaging setup with expanded probe beam [8,9]. In Fig. 5(a)–(d) are shown the spatial distribution of the intensity of focused THz pulses on the focal plane at different times [8]. At $t = 0$ ps. which corresponds to the peak of the temporal waveform observed at the center, the spatial profile is smooth and has a single peak at the center. On the other hand, at negative and positive times, we observe ring-like profile. The observed behavior was reproduced by simulations using the diffraction integral, as shown in Fig. 5(e)–(h). It was shown that the appearance of the ring-like profile is unique for the half-cycle waveform of the pulses, and it can be explained by

taking into account the frequency-dependent diffraction effects. Interestingly, similar behavior was also observed on the propagation distance dependence of the spatial profile [8]. Knowledge on these behaviors are important for the implementation of real-time THz imaging [10,17].

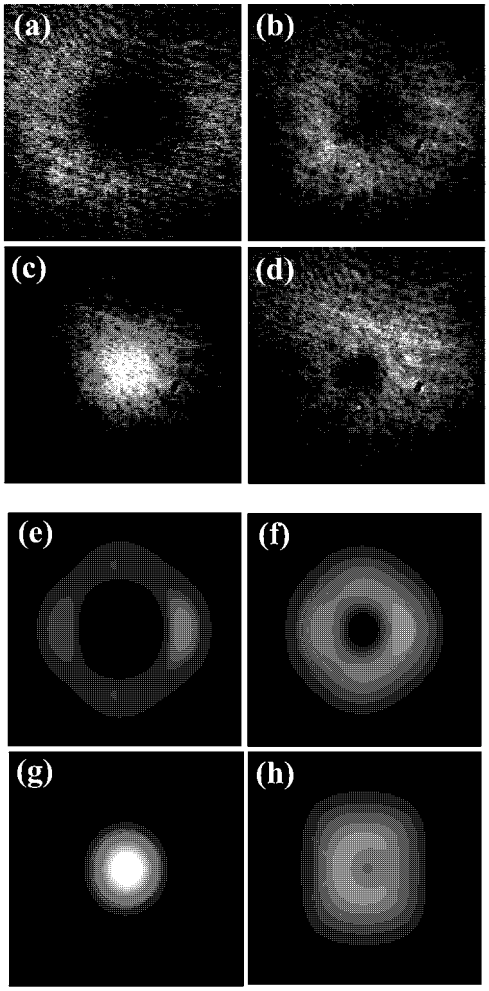

Fig. 5. (a)–(d): Experimentally obtained intensity distribution of focused THz pulses on the focal plane at different times; (a) $t = -0.72$ ps, (b) $t = -0.48$ ps, (c) $t = 0$ ps, and (d) $t = 0.4$ ps. (e)–(h): THz intensity profiles obtained by simulation based on diffraction integral at times corresponding to those of (a)–(d), respectively. Each image corresponds to an area of 12×12 mm^2 at the EO crystal.

4 Electron dynamics in GaAs and InP

Ultrafast dynamics of carriers in semiconductors is of great importance for understanding the basic physics and for applications of semiconductors in high-speed electronic devices, and has been studied extensively with various ultrafast nonlinear spectroscopic techniques, such as pump-probe and four-

wave mixing measurements [18]. Recently, techniques for generation and detection of terahertz (THz) electromagnetic radiation using femtosecond optical pulses have been developed [5,11,8,16], and are widely used in spectroscopy and imaging. In these applications, biased or unbiased semiconductors are most often used as the emitter material. In these emitter materials, transient current generated by ultrashort optical pulses serves as the source of the THz radiation. This implies that the magnitude and the temporal waveform of the emitted THz pulses carry rich information on the ultrafast dynamics of the coherent motions of the photogenerated carriers in the emitter materials.

So far, several studies on the ultrafast electron dynamics using the THz emission technique have been reported [19–22]. In these studies, electron velocity dynamics in GaAs under relatively high bias field (typically several tens of kV/cm) were observed by applying a voltage to the sample with very narrow electrode spacing (0.5–4 μm). In the present study, we adopted a different structure, a large-aperture photoconductive antenna, as the THz emitter, and observed the ultrafast dynamics of the mobility of photogenerated electrons in GaAs and InP under moderate electric field.

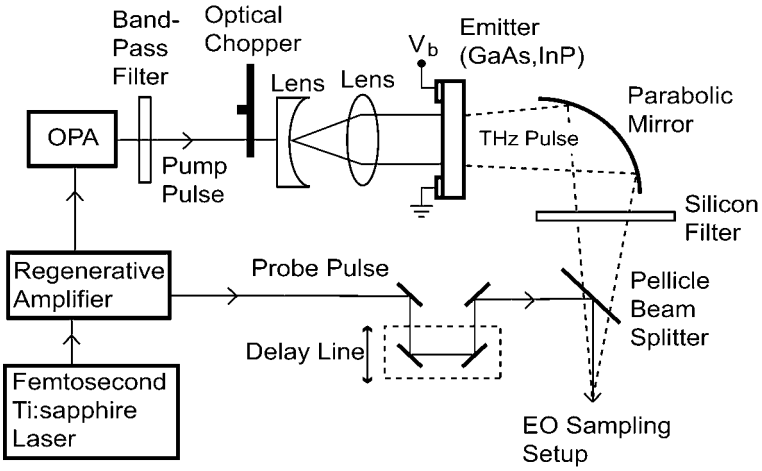

Fig. 6. Schematic of the experimental setup for the THz waveform measurement. OPA is for an optical parametric amplifier.

4.1 Experiments

A schematic for the experimental setup is shown in Fig. 6. Briefly, a GaAs or InP large-aperture photoconductive antenna [5,11] with a 3-cm gap between the electrodes was pumped at a repetition rate of 1 kHz by 150-fs tunable optical pulses obtained from an optical parametric amplifier (OPA). The temporal waveform of the electric field of the emitted THz radiation was measured using a standard setup [15] of the EO sampling method. The pump photon energy

was tuned across the band gap energy of each material; 1.428 eV for GaAs and 1.351 eV for InP. The spectral width of the pump pulse was narrowed to 10 nm using a band-pass filter. The pulse energy of the pump pulse was about 3 μJ. The photogenerated electron density is estimated to be 10^{15} to 10^{17} cm^{-3}, depending on the absorption coefficient at the pump wavelength. The probe pulse of the EO sampling measurement was obtained by splitting off a small part of the output of the regenerative amplifier, which was the seed of the OPA. The pulse width and the wavelength of the probe pulse were 130 fs and 800 nm, respectively. A silicon wafer was placed in the path of the THz radiation in order to block light and pass only THz waves. The pump pulse train was chopped at 500 Hz and the EO sampling signal was lock-in detected at this frequency.

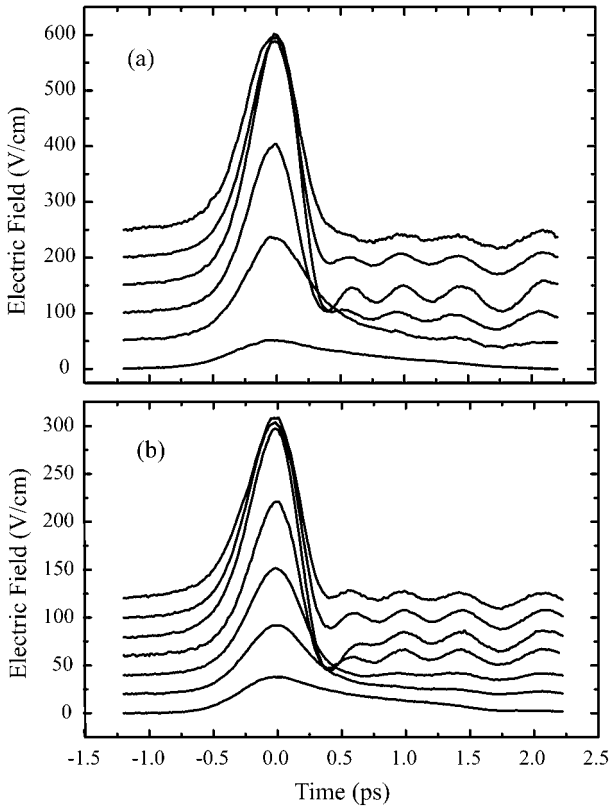

Fig. 7. Temporal waveforms of the THz pulses emitted from (a) GaAs and (b) InP for several values of the excess pump photon energy with respect to the band gap energy. The bias electric field applied to the emitter material was kept at 6.7 kV/cm. In (a), waveforms are shown for excess energies of 122, 66, 14, −3, −19, and −35 meV from the top to the bottom. Each plot is shifted upward by 50 kV/cm. In (b), waveforms are shown for excess energies of 198, 108, 11, −3, −18, −32, and −46 meV from the top to the bottom. Each plot is shifted upward by 20 kV/cm.

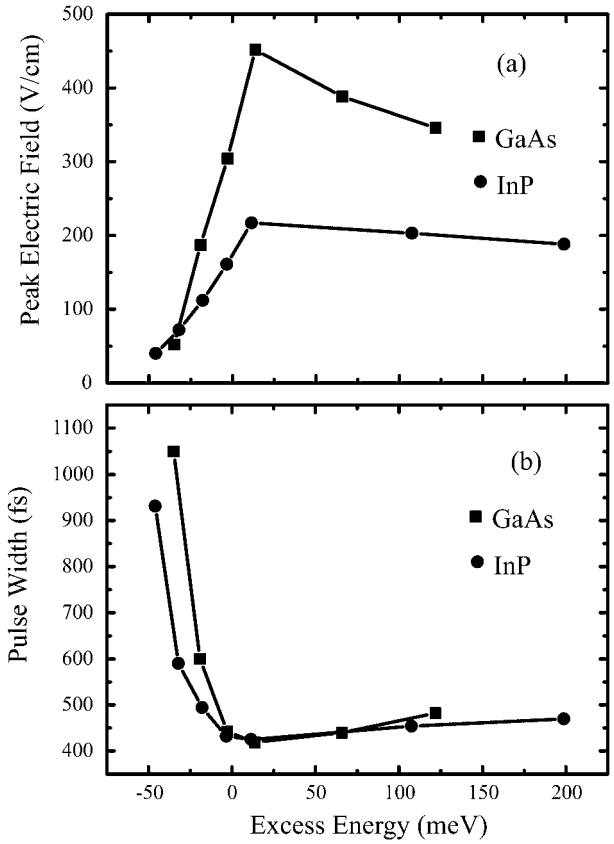

Fig. 8. The peak electric field and the temporal width of the emitted THz pulses are plotted as a function of the excess energy in (a) and (b), respectively, for GaAs (square) and InP (circle).

4.2 Results and Discussion

Pump photon energy dependence of the THz waveforms is shown in Fig. 7. The observed tendency is summarized in Fig. 8, where the peak electric field magnitude and the pulse width of the THz pulse are plotted as functions of the excess energy (pump photon energy minus band gap energy). When keeping in mind that the pump pulse has a spectral width of about 15 meV, it is seen that the largest field and shortest pulse width are obtained in both GaAs and InP when pumped by optical pulses with photon energy just above the band gap energy. The excess energy dependence of the peak field and the pulse width show a dramatic change when the sign of the excess energy is changed.

For positive excess energies, the peak field is slightly decreased and the pulse width is slightly increased for larger excess energies. The observed THz waveform can be regarded as the time derivative of the time dependence of the transient current induced by the photogeneration of electrons in the emitter materials [11]. Any contribution of photogenerated holes to the current can be neglected since the mobility of holes is much smaller. Electrons generated

in the conduction band with large excess energy have smaller mobility than at the bottom of the band, due to a larger scattering rate, and relax to the bottom on a subpicosecond timescale [18]. Correspondingly, the electron mobility is expected to increase on the same time scale [13], resulting in a slower rise of the current, or a broader THz pulse width. In contrast, when generated by pump light with photon energy slightly larger than the band gap energy, electrons are created directly at the bottom of the conduction band, leading to an almost pulse width limited rise time of the mobility. Thus, we obtained the shortest and highest THz pulse at this pump photon energy.

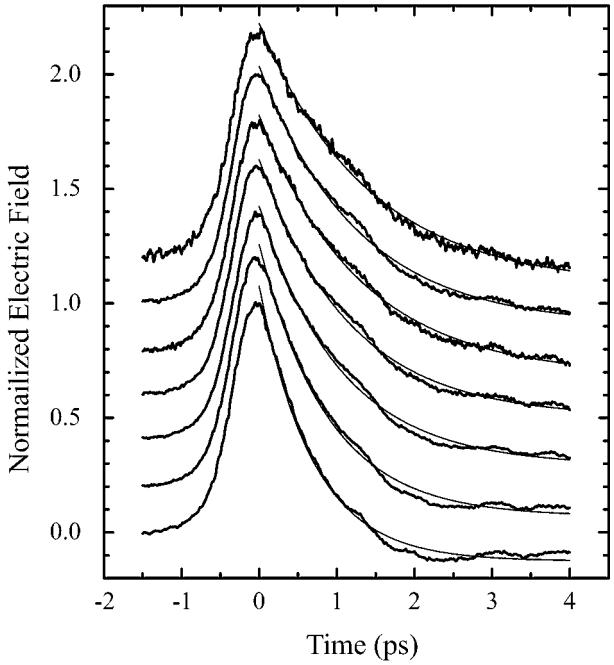

Fig. 9. Thick lines show the bias field dependence of the temporal waveforms of the THz pulses emitted from GaAs pumped with an excess energy of −35 meV. The values of the bias field are 1.3, 2.7, 4.0, 5.3, 6.7, 8.0, and 9.3 kV/cm from the top to the bottom. Thin lines show the fit of the decaying part to an exponential function. Each plot is shifted upward by 0.2.

With negative excess energies, on the other hand, we observed an exponentially decaying tail in the THz waveforms with a time constant of 1–2 ps, which corresponds to a slower rise in the mobility of electrons photogenerated in this energy region. This energy region corresponds to the Urbach tail [23], where the absorption coefficient decreases exponentially with photon energy. The Urbach tail is generally attributed to disorder in the electron potential due to electron-phonon interaction and/or defects and impurities in the crystal. The present experimental results show that the electrons excited in the Urbach tail region (Urbach electrons) do not contribute to the macroscopic current just after the excitation, and that a transition to a mobile state occurs in 1–2 ps. We believe that the present results are the first experimental observation of the ultrafast dynamics of Urbach electrons.

Furthermore, we have found that this dynamical behaviour depends sensitively on the applied bias field in the moderate field magnitude region of several kV/cm. The bias field dependence of the THz waveform emitted from GaAs with excess energy of −35 meV is shown in Fig. 9. Similar results have been obtained with InP. It is seen that the decay of the THz field becomes faster for larger bias fields. The decay times obtained by exponential fitting were 1.4 and 0.7 ps for bias fields of 1.3 and 9.3 kV/cm, respectively. Dow and Redfield [24] explained the Urbach tail formation by electric-field ionization of excitons and estimated the average effective field magnitude due to electron-LO-phonon interaction at 6.9 kV/cm in GaAs, which lies in the observation range of the present study. The fact that a large field dependence of the THz decay time has been observed in this field region in the present study shows that the observed current dynamics corresponds to thermal excitation of electrons trapped in a random potential well made by interaction with LO phonons to free carrier states.

5 Conclusion

We have first studied the behaviors of the temporal and spatial profiles of almost half-cycle THz pulses emitted from a large-aperture photoconductive antenna. The results supply the basis for the electron dynamics study of the emitter materials. We then studied the ultrafast dynamics of electrons photogenerated with positive and negative excess energies in GaAs and InP by observing the waveform of the emitted THz radiation. Subpicosecond intraband relaxation was observed with positive excess energies. With negative excess energies, picosecond transition from the Urbach state to free carrier states was observed. This dynamical behavior was found to be very sensitive to the field magnitude in the range of several kV/cm.

Acknowledgements

This study was partly supported by 21st Century Center of Excellence Program "Promotion of Creative Interdisciplinary Materials Science for Novel Functions."

References

[1] D.H. Auston, K.P. Cheung, P.R. Smith, Picosecond photoconducting Hertzian dipoles, Appl. Phys. Lett. 45 (1984) 284–286.

[2] D.R. Dykaar, S.L. Chuang, Terahertz electromagnetic pulse generation, physics, and applications: Introduction, J. Opt. Soc. Am. B 11 (1994) 2454–2456.

[3] D. You, R.R. Jones, P.H. Bucksbaum, D.R. Dykaar, Generation of high-power sub-single-cycle 500-fs electromagnetic pulses, Opt. Lett. 18 (1993) 290–292.

[4] E. Budiarto, J. Margolies, S. Jeong, J. Son, J. Bokor, High-intensity terahertz pulses at 1-kHz repetition rate, IEEE J. Quantum Electron. 32 (1996) 1839–1846.

[5] T. Hattori, K. Tukamoto, H. Nakatsuka, Time-resolved study of intense terahertz pulses generated by a large-aperture photoconductive antenna, Jpn. J. Appl. Phys. 40 (2001) 4907–4912.

[6] R.R. Jones, D. You, P.H. Bucksbaum, Ionization of Rydberg atoms by subpicosecond half-cycle electromagnetic pulses, Phys. Rev. Lett. 70 (1993) 1236–1239.

[7] D.J. Cook, J.X. Chen, E.A. Morlino, R.M. Hochstrasser, Terahertz-field-induced second-harmonic generation measurements of liquid dynamics, Chem. Phys. Lett. 309 (1999) 221–228.

[8] R. Rungsawang, K. Ohta, K. Tukamoto, T. Hattori, Ring formation of focused half-cycle terahertz pulses, J. Phys. D 36 (2003) 229–235.

[9] T. Hattori, K. Ohta, R. Rungsawang, K. Tukamoto, Phase-sensitive high-speed THz imaging, J. Phys. D 37 (2004) 770–773.

[10] R. Rungsawang, K. Tukamoto, T. Hattori, Electric field imaging using intense half-cycle terahertz pulses, Jpn. J. Appl. Phys. 44 (2005) 1771–1776.

[11] T. Hattori, R. Rungsawang, K. Ohta, K. Tukamoto, Gaussian beam analysis of temporal waveform of focused terahertz pulses, Jpn. J. Appl. Phys. 41 (2002) 5198–5204.

[12] J. T. Darrow, X.-C. Zhang, D. H. Auston, J. D. Morse, Saturation properties of large-aperture photoconducting antennas, IEEE J. Quantum Electron. 28 (1992) 1607–1616.

[13] A. Gürtler, C. Winnewisser, H. Helm, P.U. Jepsen, Terahertz pulse propagation in the near field and the far field, J. Opt. Soc. Am. A 17 (2000) 74–83.

[14] P.K. Benicewicz, J.P. Roberts, A.J. Taylor, Scaling of terahertz radiation from large-aperture biased photoconductors, J. Opt. Soc. Am. B 11 (1994) 2533–2546.

[15] A. Nahata. A.S. Weling, T.F. Heinz, A wideband coherent terahertz spectroscopy system using optical rectification and electro-optic sampling, Appl. Phys. Lett. 69 (1996) 2321–2323.

[16] K. Tukamoto, R. Rungsawang, T. Hattori, Propagation of focused terahertz pulses through subcentimeter-size conductive apertures, Jpn. J. Appl. Phys. 42 (2003) 1609–1613.

[17] R. Rungsawang, A. Mochiduki, S. Ookuma, T. Hattori, 1-kHz real-time imaging using a half-cycle terahertz electromagnetic pulse, Jpn. J. Appl. Phys. 44 (2005) L288–L291.

[18] A. Othonos, Probing ultrafast carrier and phonon dynamics in semiconductors, J. Appl. Phys. 83 (1998) 1789–1830.

[19] J.-H. Son, T.B. Norris, J.F. Whitaker, Terahertz electromagnetic pulses as probes for transient velocity overshoot in GaA and Si, J. Opt. Soc. Am. B 11 (1994) 2519–2527.

[20] A. Leitenstorfer, S. Hunsche, J. Shah, M.C. Nuss, W.H. Knox, Femtosecond charge transport in polar semiconductors, Phys. Rev. Lett. 82 (1999) 5140–5143.

[21] A. Leitenstorfer, S. Hunsche, J. Shah, M.C. Nuss, W.H. Knox, Femtosecond high-field transport in compound semiconductors, Phys. Rev. B 61 (2000) 16642–16652.

[22] M. Abe, S. Madhavi, Y. Shimada, Y. Otsuka, K. Hirakawa, K. Tomizawa, Transient carrier velocities in bulk GaAs: Quantitative comparison between terahertz data and ensemble Monte Carlo calculations, Appl. Phys. Lett. 81 (2002) 679–681.

[23] F. Urbach, The long-wavelength edge of photographic sensitivity and of the electronic absorption of solids, Phys. Rev. 92 (1953) 1324.

[24] J.D. Dow, D. Redfield, Toward a unified theory of Urbach's rule and exponential absorption edges, Phys. Rev. B 5 (1972) 594–610.